

RI 9446

REPORT OF INVESTIGATIONS/1993

In Situ Stress Measurements Near the Ross Shaft Pillar, Homestake Mine, South Dakota

By J. C. Johnson, W. G. Pariseau, D. F. Scott, and F. M. Jenkins

UNITED STATES DEPARTMENT OF THE INTERIOR



BUREAU OF MINES

Report of Investigations 9446

**In Situ Stress Measurements Near the Ross
Shaft Pillar, Homestake Mine, South Dakota**

By J. C. Johnson, W. G. Pariseau, D. F. Scott, and F. M. Jenkins

UNITED STATES DEPARTMENT OF THE INTERIOR

BUREAU OF MINES

Library of Congress Cataloging in Publication Data:

In situ stress measurements near the Ross shaft pillar, Homestake Mine, South Dakota / by J.C. Johnson ... [et al.].

p. cm. -- (Report of investigations; 9446)

Includes bibliographical references (p. 15).

1. Rock pressure--Measurement. 2. Rock mechanics--South Dakota--Lead Region. 3. Homestake Mine (S.D.). I. Johnson, J. C. (Jeffrey C.). II. Series: Report of investigations (United States. Bureau of Mines); 9446.

TN23.U43 [TN288] 622 s--dc20 [622'.25] 92-23496 CIP

CONTENTS

	<i>Page</i>
Abstract	1
Introduction	2
Acknowledgments	2
Geology	3
Background	5
Working hypothesis	6
Mine measurements	8
Procedures	8
Results	10
Discussion of results	12
Variability	12
Elastic moduli	13
Anisotropy	13
Data reduction using least squares approach	13
Summary and conclusions	14
References	15
Appendix A.—Overcore strain data from hollow inclusion cells	16
Appendix B.—Overcore plots from borehole deformation gauges	17

ILLUSTRATIONS

1. Plan view of 3650 level, Homestake Mine, Lead, SD	3
2. Geologic structures and overcoring locations at site 1	4
3. Geologic structures and overcoring locations at site 2	5
4. HICell assembled for installation	8
5. Calibration of BDG prior to installation	9
6. Specially designed thin-walled diamond set bits used to drill 6-in holes	9
7. Disking phenomenon, indicating high vertical stress, displayed in 6-in-diameter core taken 5 to 10 ft from opening.	9
8. Horizontal configuration for drilling in drift	9
9. Connecting overcored HICell to strain indicator to conduct biaxial chamber test	10
A-1. Overcore readings from HICells	16
B-1. Response of BDG to mining, site 1	17

TABLES

1. Best fit stress components for each test at sites 1 and 2	10
2. Best fit principal stresses for each test at sites 1 and 2	11
3. Average cartesian stress components from sites 1 and 2	12
4. Principal stresses from averaged and pooled results	12
5. Different axial strain treatments and results from site 2	14
6. Stresses near Ross shaft pillar at sites 1 and 2	15

UNIT OF MEASURE ABBREVIATIONS USED IN THIS REPORT

deg degree

pct percent

ft foot

psi pound per square inch

in inch

IN SITU STRESS MEASUREMENTS NEAR THE ROSS SHAFT PILLAR, HOMESTAKE MINE, SOUTH DAKOTA

By J. C. Johnson,¹ W. G. Pariseau,² D. F. Scott,³ and F. M. Jenkins⁴

ABSTRACT

In situ stresses are important input data for the design of safe, stable stope layouts and extraction sequences. However, it is commonly assumed that normal and shear stress gradients in a stress field are negligible and, consequently, that stresses are uniform throughout the region of analysis. To evaluate these assumptions and to provide input data for an analysis of a shaft pillar mining plan, in situ stresses were measured at the Homestake Mine, Lead, SD, using overcoring on hollow inclusion cells and borehole deformation gauges.

These measurements were used with conventional least squares, best fit data reduction schemes. The results showed that normal stresses within the shaft pillar were less than, but comparable to, those estimated from finite-element modeling. Shear stresses were an order of magnitude less than normal stresses and varied considerably from site to site. Possible causes of this variability include effects of scale, elastic moduli, anisotropy, and axial strain. Because of the variability, it is not possible to determine the magnitude of horizontal stress gradients.

¹Mining engineer, Spokane Research Center, U.S. Bureau of Mines, Spokane, WA.

²Mining engineer, Spokane Research Center; McKinnon professor of mining engineering, University of Utah, Salt Lake City, UT.

³Geologist, Spokane Research Center.

⁴Staff engineer, Division of Health, Safety, and Mining Technology, U.S. Bureau of Mines, Washington, DC.

INTRODUCTION

The U.S. Bureau of Mines and the Homestake Mining Co. are engaged in a cooperative effort involving studies of rock mechanics and the stability of pillar mining near the Ross shaft at the Homestake Mine, Lead, SD. The project is part of Bureau research into advanced concepts for modern mine design in support of the Bureau's goal to enhance recovery of the Nation's mineral resources. The research goal is to advance design technology in the complex three-dimensional realm of underground hard-rock mining.

Large-scale, catastrophic motion about a shaft is clearly unacceptable. However, shaft wall displacements that can be accommodated operationally without serious interruption of the hoisting schedule may be tolerable. Thus, the key to a successful engineering plan for shaft pillar mining is to ensure that movement in a rock mass is within expectations.

An effective approach to studying rock mass movement combines laboratory testing for rock properties, numerical modeling and simulations of various pillar extraction sequences, measurements of stress and displacement in a mine, and monitoring shaft reactions to mining. Measurements and monitoring provide data for model validation, calibration, review, revisions, and possible extension of the model from two to three dimensions. A simple model is preferred at the outset, but when mine measurements and monitoring data indicate that the complexities of mine geology and mine geometry require a more comprehensive model, then revisions and extensions are necessary.

The Ross shaft pillar is in high-grade ore on the west side of the shaft and extends 100 ft north and south of the shaft. Vertical extent is indefinite. Extensive mining in the past led to the formation of the shaft pillar and undoubtedly modified the original stress field about the Homestake Mine. Stress measurements in the pillar provided the data needed to compare the results of finite-element simulations of historical mining to the present (posthistorical, prepillar mining) stress state. The present stress state is important because future mining in the pillar and model simulations depend on the stresses at the start of pillar mining.

This Report of Investigations is the first of several related to the Ross shaft pillar study. It discusses the results of stress measurements taken at two sites on the 3650 level of the Homestake Mine, where a large percentage of the shaft pillar ore is found. Site 1 (fig. 1) is located near the center of the Ross pillar about 250 ft west of the shaft and 20 ft south of the shaft centerline. Site 2 (fig. 1) is located approximately 750 ft southeast of site 1 in a relatively remote region of the mine.

The immediate objectives were to determine (1) the present state of stress in the Ross shaft pillar and (2) the horizontal stress gradients in the same area. The overall objective was to advance the state of the art of mine design. The Homestake Mine site provided an opportunity for full-scale testing of concepts that have industry-wide applicability.

ACKNOWLEDGMENTS

The in situ stress measurement project involved the efforts of many people. Special thanks go to management and technical personnel at the Homestake Mine, particularly Al Winters and Carl Schmuck, who provided access to the mine, and to Wayne Corso, who provided

engineering support. Thanks also go to Dave Benjamin and Paul Hyndman of the Bureau's Western Field Operations Center, Spokane, WA, who assisted with mapping the geology of the mine sites.

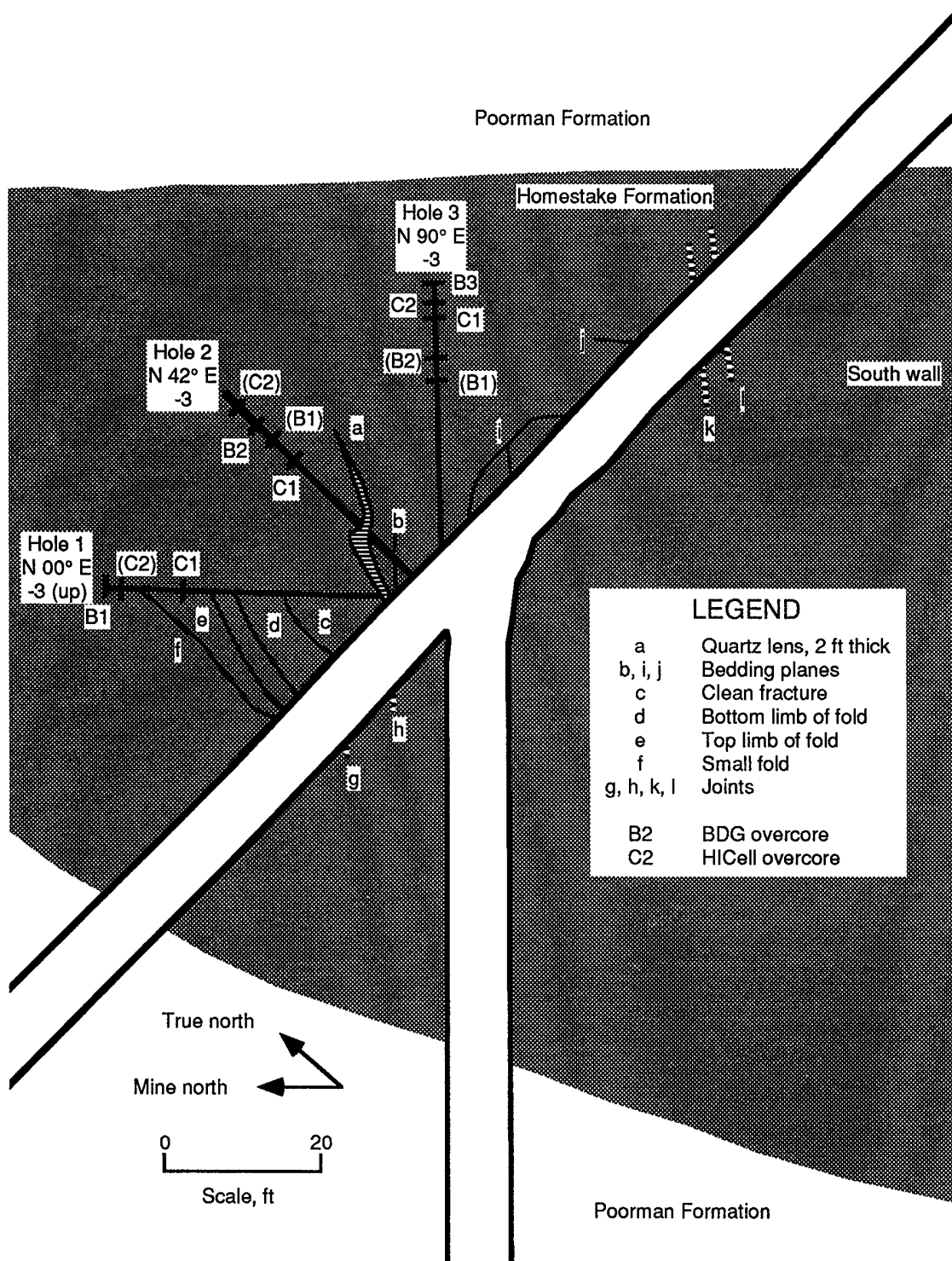


Figure 2.—Geologic structures and overcoring locations at site 1.

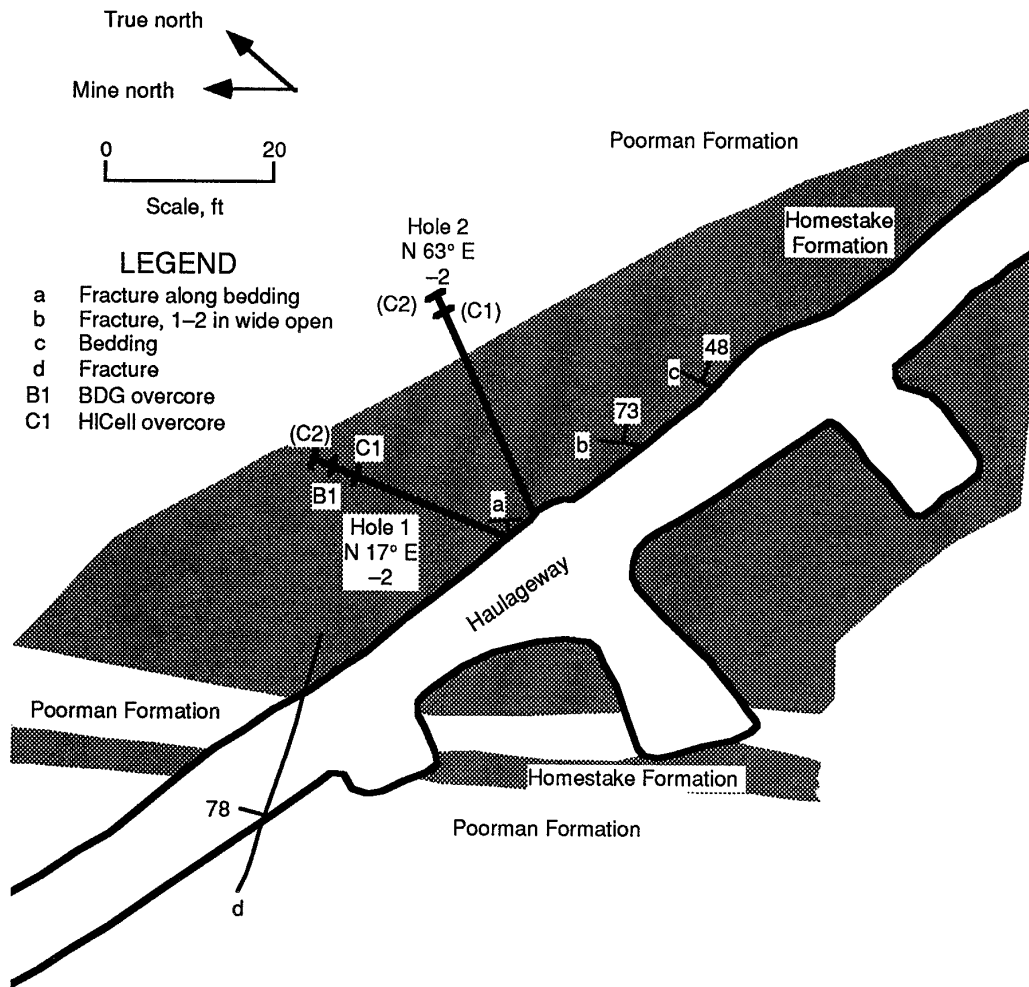


Figure 3.—Geologic structures and overcoring locations at site 2.

BACKGROUND

In situ, or premining, stresses are the loads applied to excavations in rock. These stresses play a major role in numerical analyses of the safety and stability of mine openings. It is therefore important to determine premining stresses as accurately as possible within the practical constraints of cost and data variability.

In situ stress measurements require specially trained personnel and equipment and are relatively expensive to obtain. The cost often limits the number of measurements to those that can be taken from boreholes collared from a single drill station. Mapping a highly variable in situ stress field over a large region is not practical despite advances in equipment and techniques that allow three-dimensional stress states to be determined from a single

gauge. However, if the premining stress field is homogeneous, then a single, reliable stress measurement is sufficient to define the in situ stress field. The difficulty is that stress field homogeneity, or lack of it, cannot be known until a sufficient number of measurements are made.

In practice, the number of measurements actually collected is usually far less than what is needed for achieving a high confidence level in statistical analyses. The reason is large measurement variability. In the present context, variability refers to differences in the outcome of in situ stress measurements and is closely linked to heterogeneity of the rock mass as well as experimental error. Rock mass heterogeneity ranges from laboratory-sized test

specimens taken from a borehole or from rock masses the size of an ore body or larger. Thus, variability occurs over a multiplicity of scales and reflects interactions among applied load, geologic structure, and rock type. Applied loads are primarily gravitational and tectonic.

Pair-wise differences are commonly observed among stress measurements (1) from the same borehole, (2) from different boreholes at the same drill site, (3) from different drill sites on the same level, and (4) from drill sites on different levels in the same mine. Such differences may result from differences in the types of gauges used or data reduction procedures, as well as actual differences in *in situ* stresses.

Over distances of about 1,000 ft, approximately the linear dimension of a finite-element model of a typical hard-rock mine stope, it may be practical to take into account stress field changes. Thus, a difference in stress between two sites may be important in constructing a numerical model if the distance between these sites is about the same as the linear dimensions of the area of the mine being modeled. For example, a finite-element model of a stope in a mine where levels are 150 ft apart would be about 1,000 ft high. A reasonable assumption would be that the vertical stress gradient caused by gravity loading alone would be about 1.2 psi per foot of depth. The

difference in the vertical stress component (gravity) between the top and bottom of the model would then be about 1,200 psi. If the stope were centered in a moderately deep mine, say, at the 3600-ft level, then the difference in vertical stress between the top and the bottom would be more than 25 pct of the vertical stress at the center of the stope. If the same stope were centered at the 7200-ft level, the difference would only be about 13 pct and perhaps of no great concern.

Horizontal gradients in stress should also be considered in numerical analyses of mine opening stability. However, there appears to be little discussion in the technical literature of how horizontal stress gradients might be incorporated into such an analysis. When considering vertical stress gradients, there is a simple physical basis for determination, that is, gravity loading. The situation is much less clear for horizontal gradients where the specific physical cause is not known. Measurements must then be relied upon to reveal the presence of horizontal stress gradients. However, if the differences in stresses between sites about 1,000 ft apart horizontally are similar to the differences between measurements taken from the same borehole or at the same site, then it is questionable whether there is any justification for including horizontal stress gradients in a model analysis.

WORKING HYPOTHESIS

A simple hypothesis for approaching the problem of determining stress gradients is to consider the model region as the neighborhood of a mathematical point. Let the state of stress σ at point x_0, y_0, z_0 and time t_0 be characterized by the six independent components $\sigma_{xx}, \sigma_{yy}, \sigma_{zz}, \sigma_{xy}, \sigma_{yz}, \sigma_{zx}$ of the stress tensor referred to a fixed cartesian coordinate system. The stress field at nearby point x, y, z and later time t may be estimated from known data by a Taylor series expansion (equation 1) about the given point. Thus,

$$\begin{aligned} \sigma(x, y, z, t) = & \sigma(x_0, y_0, z_0, t_0) + (\partial\sigma/\partial x)dx + (\partial\sigma/\partial y)dy \\ & + (\partial\sigma/\partial z)dz + (\partial\sigma/\partial t)dt \\ & + \text{higher order terms,} \end{aligned} \quad (1)$$

where σ represents any one of the six stress components. The derivatives in equation 1 are evaluated at the given point.

If the *in situ* stress state varies slowly over geologic time, then

$$(\partial\sigma/\partial t) = 0 \quad (2)$$

over the time spans of engineering interest, and only spatial variations in the *in situ* stress field need to be determined. Negligible variations over time are implied in most *in situ* stress measurements, although time-dependent, postmining stress changes are considered in some cases, for example, in salt mines. Lateral variation is also considered negligible in most determinations of the premining stress state.

The change in stress $\Delta\sigma$ between x, y, z and x_0, y_0, z_0 is

$$\Delta\sigma = (\partial\sigma/\partial x)dx + (\partial\sigma/\partial y)dy + (\partial\sigma/\partial z)dz. \quad (3)$$

The smaller the stress gradients $\partial\sigma/\partial x$, $\partial\sigma/\partial y$, and $\partial\sigma/\partial z$, the greater the distance (as measured by dx , dy ,

dz) must be between points before a significant change in stress occurs. From equation 1,

$$\Delta\sigma = \sigma(x,y,z) - \sigma(x_0,y_0,z_0). \quad (4)$$

If stress measurements are made at four sites that are not all in the same plane, then equations 3 and 4 can be solved for the stress gradients. In matrix notation, the system of equations is

$$\{\Delta\sigma\} = [d]\{\partial\sigma\}, \quad (5)$$

where $\{\Delta\sigma\} = (\Delta_1\sigma \ \Delta_2\sigma \ \Delta_3\sigma)^t$ and is a 3- by 1-column matrix of stress changes between the original site and each of the three additional sites 1, 2, and 3. The parentheses imply a 1- by 3-row matrix, superscript t means to transpose, and $\{\partial\sigma\} = (\partial\sigma/\partial x \ \partial\sigma/\partial y \ \partial\sigma/\partial z)^t$ and is a 3- by 1-column matrix of the unknown spatial gradients of a stress component. The coefficient matrix $[d]$ contains the coordinate distances between measurement sites.

$$[d] = \begin{bmatrix} x_1-x_0 & y_1-y_0 & z_1-z_0 \\ x_2-x_0 & y_2-y_0 & z_2-z_0 \\ x_3-x_0 & y_3-y_0 & z_3-z_0 \end{bmatrix}, \quad (6)$$

where $x_1,y_1,z_1 =$ coordinates of measurement site 1 and so forth. Equation 5 must be solved for the spatial gradients of each of the six stress components.

Once all the stress gradients are known, a stress component in the model at arbitrary point x,y,z is given by the linear form

$$\sigma = a_0 + a_1x + a_2y + a_3z, \quad (7)$$

where the coefficients are known constants. Equation 7 remains the same with a change in the origin of the coordinates. Thus, the in situ stresses are given in matrix notation as

$$\{\sigma\} = [c]\{p\}, \quad (8)$$

where $\{\sigma\} = (\sigma_{xx} \ \sigma_{yy} \ \sigma_{zz} \ \sigma_{xy} \ \sigma_{yz} \ \sigma_{zx})^t$ and is a 6- by 1-column matrix; $[c]$ = the coefficient matrix; $\{p\} = (1 \ x \ y \ z)^t$ and is a 4- by 1-column matrix; and x,y,z are coordinates with respect to a new origin (x_0,y_0,z_0) relative to the original measurement site. The possibility of using a new origin point is a modeling convenience.

The coefficient matrix $[c]$ contains stress gradient information determined previously and has the dimensions of a 6 by 4 matrix. The coefficients in typical row r of $[c]$ are

$$c_{r1} = \sigma_0 + (\partial\sigma/\partial x)_0x_0 + (\partial\sigma/\partial y)_0y_0 + (\partial\sigma/\partial z)_0z_0, \quad (9a)$$

$$c_{r2} = (\partial\sigma/\partial x)_0, \quad (9b)$$

$$c_{r3} = (\partial\sigma/\partial y)_0, \quad (9c)$$

$$\text{and } c_{r4} = (\partial\sigma/\partial z)_0, \quad (9d)$$

where the stress gradients are determined from equation 5 and the subscript 0 implies evaluation with respect to the original measurement site. The evaluations are simple arithmetic calculations using measurement data.

Equation 8 allows for a simple assignment of initial (premining) stresses to all elements in a finite-element model. For example, when linear displacement (constant strain) elements are used, the coordinates x,y,z are simply the coordinates of an element centroid, σ_0 is the measured state of stress at point x_0,y_0,z_0 , and the gradients are derived from equation 5. If horizontal stress gradients are absent, then

$$\sigma_{xx} = [\sigma_{xx0} + (\partial\sigma_{xx}/\partial z)_0z_0] + (\partial\sigma_{xx}/\partial z)z. \quad (10)$$

The other five stress components are calculated in a similar manner.

In a homogenous rock mass loaded by gravity only, the premining shear stresses are zero, and further simplification of equation 8 is possible. Only the vertical and two horizontal stresses and their vertical gradients remain. Thus, the premining stress state must be given by

$$\sigma_v = a_1 + b_1z, \quad (11a)$$

$$\sigma_H = a_2 + b_2z, \quad (11b)$$

$$\text{and } \sigma_h = a_3 + b_3z, \quad (11c)$$

where $a_1, a_2,$ and a_3 correspond to the constant terms in brackets in equation 10; $b_1, b_2,$ and b_3 correspond to the gradient terms; subscript v = vertical; and subscripts H and h = horizontal and are mutually perpendicular. Under the simplified conditions of gravity loading only and a

homogeneous rock mass, the normal stresses in equation 11 are principal stresses. Thus, with compression positive,

$$\sigma_v = \sigma_1, \quad (12a)$$

$$\sigma_H = \sigma_2, \quad (12b)$$

and
$$\sigma_h = \sigma_3. \quad (12c)$$

At the Homestake Mine, an analysis of previous stress measurement data (*I*)⁵ leads to the calculations

$$\sigma_v = 1.25 z, \quad (13a)$$

$$\sigma_H = 2,078 + 0.53 z, \quad (13b)$$

and
$$\sigma_h = 121 + 0.55 z, \quad (13c)$$

where z = depth below ground surface. These calculations are consistent with simplified equation 11 and suggest vertical loading by gravity only, but with horizontal loads in excess of those caused by gravity alone. At the 3650 level near the Ross shaft pillar, the stresses calculated from equation 13 are $\sigma_v = 4,563$ psi, $\sigma_H = 4,013$ psi, and $\sigma_h = 2,129$ psi.

The in situ stress hypothesis represented by equation 9 assumes linear premining stress gradients and implies that the stress gradients are independent of position. Thus, a linear regression analysis is an alternative approach to defining the coefficients in equation 9. A companion analysis of variance of measurements taken within a given site and between sites could also be done, provided that the number of measurements justified a statistical approach. Unfortunately, this is seldom the case.

MINE MEASUREMENTS

The stress relief overcoring method was used for all stress measurements. Hollow inclusion cells and borehole deformation gauges were used to provide a check on results. Difficulties in gauge cement and biaxial chamber tests were encountered. The working environment was severe; time prevented taking as many measurements as desired.

PROCEDURES

Nearly horizontal 1.5-in-diam boreholes were drilled about 30 ft deep at each site. Drift dimensions near the measurement sites are about 20 ft wide by 10 ft high. Thus, to reduce the influence of stress concentration at a gauge site, the first gauge was installed 20 ft into a hole.

Commonwealth Scientific and Industrial Research Organization (CSIRO) hollow inclusion cells (HICells)⁶ (fig. 4) and the Bureau's borehole deformation gauge (BDG) (fig. 5) were used to collect all stress measurements. The HICell contains three three-gauge strain rosettes and allows for the determination of the three-dimensional stress state from a single overcore. The BDG requires three overcores, one each in three nonparallel boreholes. Gauges of both types were installed in boreholes at site 1, but only two boreholes were drilled at site 2.

⁵Italic numbers in parentheses refer to items in the list of references preceding the appendixes at the end of this report.

⁶Reference to specific products does not imply endorsement by the U.S. Bureau of Mines.

The location of all gauges and holes at site 1 and site 2 are shown in figures 2 and 3, respectively. Installation and data reduction were according to procedures described in references 2 and 3. After gauge installation, stress relief was obtained by overcoring (figs. 6-7). Figure 8 shows the drill station in a drift. Strain measurements were continuously recorded during the overcoring process. A heating unit was used to maintain drill water at a constant temperature during overcoring and thus prevent spurious thermal strains from appearing in the measurements.

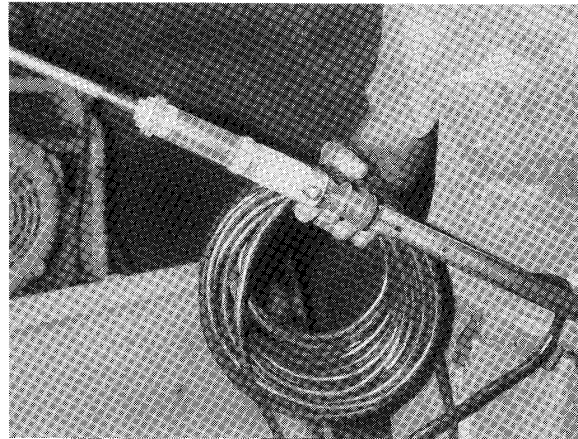


Figure 4.—HICell assembled for installation. When forced to the bottom of prepared hole, rod and plunger extrude epoxy to bond device to rock.

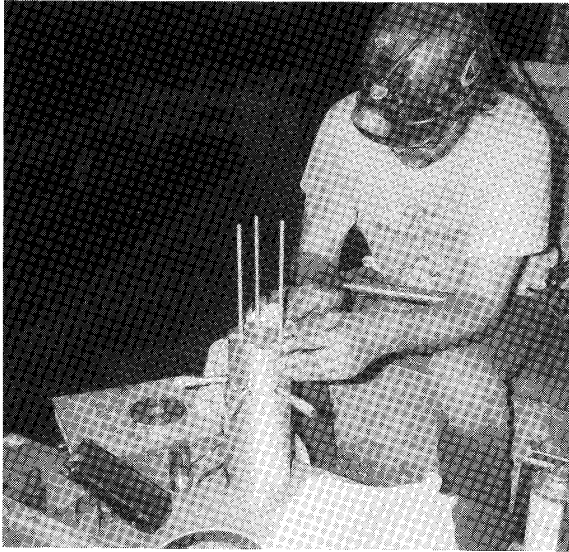


Figure 5.—Calibration of BDG prior to installation. Instruction manual must be followed carefully to ensure accurate results.

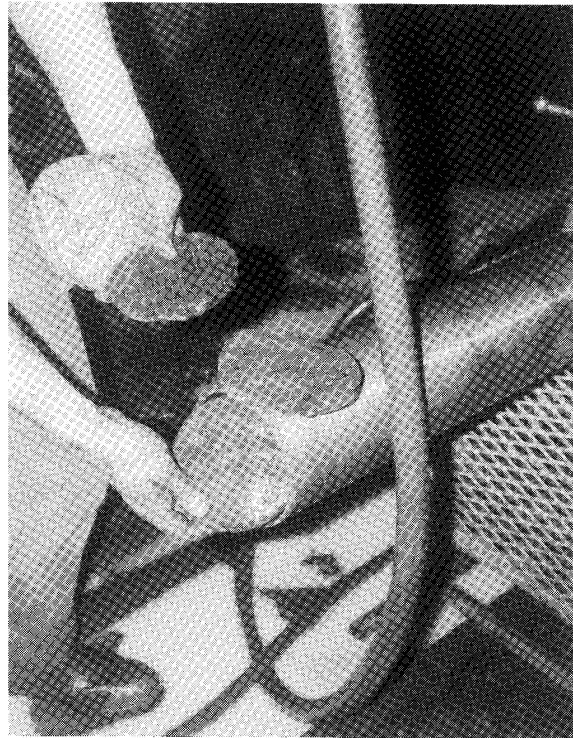


Figure 7.—Disking phenomenon, indicating high vertical stress, displayed in 6-in-diameter core taken 5 to 10 ft from opening.

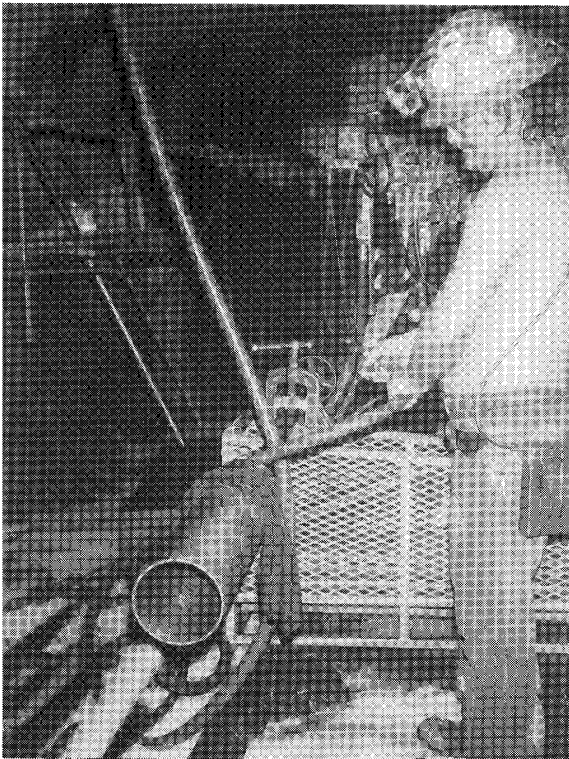


Figure 6.—Specially designed thin-walled diamond set bits used to drill 6-in holes. Both HICell and BDG were alternately installed and overcored in same holes.

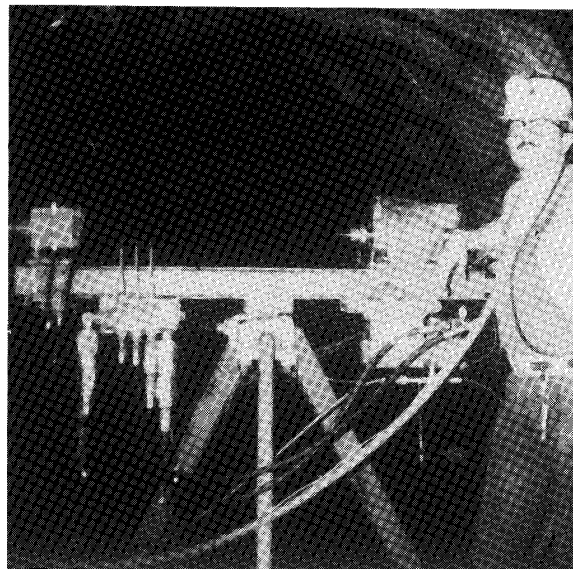


Figure 8.—Horizontal configuration for drilling in drift. An experienced driller is needed at the controls.

Six HICells and six BDG's were installed at site 1; of these, four HICells and three BDG's were successfully overcored. Appendix A contains plots of all successful HICell overcore strain measurements. HICell gauge response during overcoring appears normal with the exception of gauge 9, where oscillations in the data were probably caused by a fault in the recording channel. Fortunately, gauge 9 was a redundant angle gauge. Appendix B contains plots of the BDG overcoring data.

Four HICells were installed at site 2, but only one was successfully overcored. Sectioning the retrieved HICell overcores with the gauges still in place showed that the failures were caused by air bubbles in the gauge cement and improper bonding of the gauge to the borehole wall. Because three nonparallel boreholes are needed to obtain sufficient data from a BDG to estimate the stress state and only two boreholes were drilled, it was not possible to determine stresses with the BDG at site 2.

Biaxial testing of HICell overcores for Young's modulus and Poisson's ratio also proved troublesome; only a single test was completed. Partial data were obtained from four other overcores, including the results of two uniaxial tests. As a consequence, the estimate of Young's modulus needed for data reduction was highly uncertain. Anisotropy added to the uncertainty; this topic is discussed in the "Anisotropy" section. Figure 9 shows a biaxial test being performed in the mine.

RESULTS

The in situ stresses were calculated from measured HICell strains and BDG displacements using a data reduction program modified by Larson (4). Both the manufacturer's original program and the modification by Larson

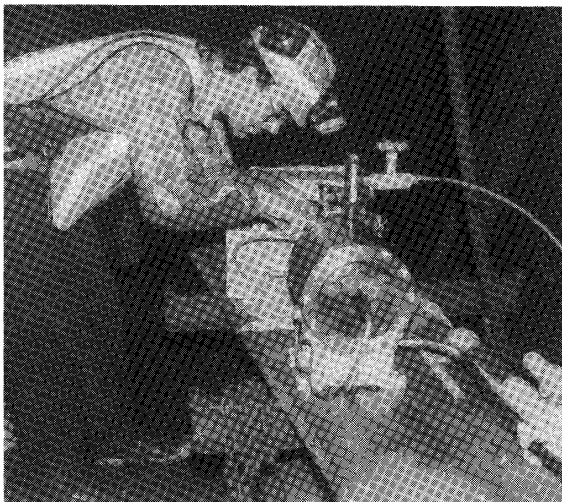


Figure 9.—Connecting overcored HICell to strain indicator to conduct biaxial chamber test.

assume linearly elastic and isotropic rock behavior. Both use a multiple variable linear regression model to find a best fit to the HICell strain measurements. This approach views the nine HICell strain measurements available for determination of the six independent components of stress as an overdetermined system and successively eliminates three redundant gauge measurements to obtain the best fit or the solution with the least variance. Only redundant measurements may be eliminated. For example, only one of the two axially positioned gauge measurements can be discarded in the process of seeking a best fit.⁷ A similar approach was applied to the BDG measurements of borehole wall displacement.

The best-fit cartesian components of stress obtained from all HICell measurements at sites 1 and 2 and the BDG measurements at site 1 are given in table 1. The results show a consistent ordering of the normal stresses at site 1. With the exception of the measurement from S1H3C2,⁸ the vertical stress is always the largest normal stress; the east-west stress is intermediate in value; and the north-south stress is the smallest normal stress. The east-west direction is perpendicular to strike; the north-south direction is parallel to strike. The shear stresses tend to be an order of magnitude smaller than the normal stresses and vary in algebraic sign, although the north-vertical or south-vertical shear stresses from each HICell are always negative. A shear stress sign reversal implies a reversal in direction of action.

⁷A HICell has two axial gauges (1, 7), three circumferential gauges (2, 6, 8), and four angle gauges (3, 4, 5, 9) oriented at 45° to the cell axes.

⁸In the notation, the letter and the first digit indicate site, the second letter and the second digit indicate borehole, and the third letter and the third digit indicate cell. Thus S1H3C2 means site 1, borehole 3, cell 2.

Table 1.—Best fit stress components for each test at sites 1 and 2, pounds per square inch

(Compressive stress is positive)

Test	Normal			Shear		
	North-south	East-west	Ver-tical	North-south and east-west	East-west and ver-tical	North-south and ver-tical
SITE 1						
S1H1C1 ..	2,218	2,245	4,868	-327	344	-67
S1H2C1 ..	2,674	2,771	3,551	92	-171	-171
S1H3C1 ..	1,962	2,419	3,838	132	1,187	-379
S1H3C2 ..	2,575	7,506	4,409	858	-1,373	-1,193
BDG	2,830	4,750	5,170	1,590	130	300
SITE 2						
S2H1C1 ..	4,238	2,321	5,153	-37	694	-715

Measurement S1H3C2 is an exception. Although the north-south normal stress is still the smallest, the vertical and east-west stresses are in reverse order relative to the other measurements from site 1. Large vertical shear stresses are also indicated, but these are about one-half the smallest normal stress.

At site 2, the vertical stress is the largest normal stress, but the north-south and east-west stresses are in reverse order. Again, large vertical shear stresses are noted.

The results in terms of principal stresses are shown in table 2. Major principal stresses (compression) range from a low of 3,623 psi at S1H2C1 to a high of 8,297 psi at S1H3C2. Intermediate principal stresses range from 1,930 to 5,065 psi; minor principal stresses range from 1,718 to 2,614 psi. Principal stresses at site 2 are near the mid-ranges of the stresses from site 1.

The major principal stress lies within 30° of vertical, so that the intermediate and minor principal stresses lie in planes within 30° of horizontal. There are two exceptions to this pattern. One is at S1H3C2, noted previously; the other was obtained from the BDG. High shear stresses in both cases rotate the major compression to within 24° of horizontal.

The data in table 2 suggest that the intermediate principal stress is oriented perpendicular to strike and that the minor principal stress is parallel to strike. The same suggestion is implicit in the cartesian stress components shown in table 1. However, variability in orientation is large, and no strong conclusions are warranted.

There are two ways to average site measurements to characterize the stress state at a given site. The first is to average the cartesian stress components arithmetically; the second is to pool all HICell strain measurements from the site and calculate a least squares fit to the pooled data. The results of both methods may be compared with the stresses calculated from finite-element modeling of past mining sequences. The difference in the average site 1 and site 2 stress states then defines the stress gradients according to the hypothesis presented earlier.

Table 3 shows the arithmetically averaged HICell data from table 1 and the same cartesian components of stress obtained from a best fit to the pooled strain data from site 1. Both sets show the same ordering of normal stresses noted previously. The vertical stress is the largest; the smallest normal stress is parallel to strike. The tendency for the shear stresses to be an order of magnitude less than the normal stresses is seen again in table 3. The averaged data from site 2 are the same as the data in table 1 because there is only a single measurement available from site 2. The finite-element modeling results follow the same trend, but show larger normal stresses than either averaged or pooled results.

Table 2.—Best fit principal stresses for each test at sites 1 and 2

(Compressive stress is positive)

Test ¹	Magnitude, psi	Orientation, deg	
		Dip direction from azimuth	Dip, +down
SITE 1			
S1H1C1:			
$\sigma_1 \dots$	4,917	287	-82
$\sigma_2 \dots$	2,522	316	7
$\sigma_3 \dots$	1,892	226	4
S1H2C1:			
$\sigma_1 \dots$	3,623	48	-73
$\sigma_2 \dots$	2,759	246	-16
$\sigma_3 \dots$	2,614	154	-5
S1H3C1:			
$\sigma_1 \dots$	4,571	73	-60
$\sigma_2 \dots$	1,930	158	3
$\sigma_3 \dots$	1,718	66	30
S1H3C2:			
$\sigma_1 \dots$	8,297	257	23
$\sigma_2 \dots$	4,212	130	55
$\sigma_3 \dots$	1,981	178	-25
BDG:			
$\sigma_1 \dots$	5,764	59	24
$\sigma_2 \dots$	5,065	69	-66
$\sigma_3 \dots$	1,921	151	4
SITE 2			
S2H1C1:			
$\sigma_1 \dots$	5,664	337	-61
$\sigma_2 \dots$	3,897	190	-25
$\sigma_3 \dots$	2,152	94	-14

¹ σ_1 = major principal stress; σ_2 = intermediate principal stress; σ_3 = minor principal stress.

The principal stresses and directions calculated from the results shown in table 3 are given in table 4. There are noticeable differences in magnitude and orientation of the principal stresses when the stresses are calculated from arithmetic averages of the cartesian components of stress and a least squares best fit to the pooled strain measurements. The numerical reason for the differences is that higher vertical shear stresses are present in the arithmetically averaged data. The finite-element principal stresses are greater than the pooled and averaged results, as expected from the cartesian information provided in table 3. Orientation of the principal stresses obtained from using the finite-element analysis is closer to the result obtained by pooling orientations, but is more closely aligned with strike than are orientations derived from either pooled or arithmetically averaged results.

Table 3.—Average cartesian stress components from sites 1 and 2, pounds per square inch

(Compressive stress is positive)

Averaged	Normal			Shear		
	North-south	East-west	Vertical	North-south and east-west	East-west and vertical	North-south and vertical
SITE 1						
Arithmetic	2,357	3,735	4,167	189	-597	-453
Pooled	2,142	2,188	3,807	-266	-222	-39
Finite-element model ..	2,577	4,882	6,135	-258	76	256
SITE 2						
Arithmetic	4,238	2,321	5,153	-37	694	-715
Pooled	4,238	2,321	5,153	-37	694	-715

Table 4.—Principal stresses from averaged and pooled results

(Compressive stress is positive)

Averaged ¹	Magnitude, psi	Orientation, deg		Averaged ¹	Magnitude, psi	Orientation, deg	
		Dip direction from azimuth	Dip, + down			Dip direction from azimuth	Dip, + down
SITE 1				SITE 2			
Arithmetic:				Arithmetic:			
σ_1	4,685	70	-54	σ_1	5,664	337	-61
σ_2	3,326	276	-33	σ_2	3,897	190	-25
σ_3	2,248	178	-13	σ_3	2,152	94	-14
Pooled:				Pooled:			
σ_1	3,837	89	-82	σ_1	5,664	337	-61
σ_2	2,420	134	5	σ_2	3,897	190	-25
σ_3	1,880	44	5	σ_3	2,152	94	-14
Finite-element model:							
σ_1	6,156	56	-82				
σ_2	4,909	174	-2				
σ_3	2,529	84	4				

¹ σ_1 = major principal stress; σ_2 = intermediate principal stress; σ_3 = minor principal stress.

DISCUSSION OF RESULTS

Factors that influence the interpretation of results include the following:

1. Factors influencing variability at different scales,
2. The numerical values of Young's modulus and Poisson's ratio used to calculate stresses from the HiCell strain measurements,
3. The assumption of isotropic rock in the Homestake Mine, and
4. The least squares, best fit data reduction procedure.

Although data are sparse and do not allow a rigorous, detailed statistical analysis, some discussion is warranted.

The last item above is a particularly interesting topic that does not appear to be addressed in the technical literature.

VARIABILITY

If other factors remain constant, differences in the stress state from a given site must be caused by heterogeneity of the rock mass along the same borehole and among boreholes collared at the same site. Geologic variability on the scale of feet induces variability among stress measurements on the same scale. Variability is properly measured within a cartesian frame; differences in principal

stresses are misleading because the orientations of the principal axes are not fixed.

There are only two HICell measurements available to study within-hole variability at site 1 and none at site 2. The measurements from site 1 indicate that the order of the largest and the intermediate normal stresses was reversed and that these stresses varied by about 50 pct from their mean stress components. The high degree of variability over a distance of several feet in the same hole brings the validity of the measurements into question. However, the results may also be an artifact of the data reduction scheme.

There are four HICell measurements available to study within-site variability at site 1. When the east-west stress measurements from S1H3C2, which are unusually high, are ignored, deviations from the arithmetic mean are about 16 pct. Stress variability at site 1 is therefore characterized by no more than a 1,300-psi spread in normal stress. Differences between high and low values of normal stress fall within this range. The spread is the same magnitude as the increase in vertical stress caused by gravity loading of a finite-element mesh about 1,100 ft high.

The contact between the Homestake and Poorman Formations may have influenced the results at site 1. Stress measurements taken on both sides of a geologic contact may shed light on how changes in rock properties affect a stress field at a material discontinuity. A fundamental issue in rock mechanics concerns such changes.

The difference in arithmetically averaged vertical stresses between sites 1 and 2 is about 1,000 psi or about ± 11 pct of the mean of the vertical stresses at the two sites. However, the between-site variability of the other normal stress is problematic because of the reversal in ordering. The situation raises questions similar to those regarding within-hole variability. As it is, the observed difference between north-south stresses is almost 2,000 psi, while the difference between the east-west stresses is 1,400 psi. The ranges are ± 44 and ± 23 pct of combined means from the two sites, respectively. Thus, horizontal stress variability, or differences between sites on the same level spaced about 750 ft apart, is somewhat greater than vertical stress variability within site 1 and between sites 1 and 2.

ELASTIC MODULI

For isotropic materials, the pertinent elastic moduli for reducing strain measurements to stresses are Young's modulus (E) and Poisson's ratio (ν). Values of 6.5×10^6 psi and 0.20 were used to obtain all results reported here. The amount of data from biaxial and other tests to establish rock properties, although limited, suggests that both values should be higher. At fixed ν , the calculated

stresses are directly proportional to E . Increasing E by 20 pct increases all stress components by 20 pct. The effect of increasing ν is more subtle. Trial calculations and comparisons at fixed E using the same set of strain measurements and a value of 0.37 for ν show an increase in normal stresses up to 18 pct, but a decrease in shear stress. The best choice of elastic moduli is complicated further by the question of anisotropy.

ANISOTROPY

The computer program that reduces HICell strain measurements to stresses is based on the assumption of isotropic rock. However, the metasedimentary formations at the Homestake Mine have directional characteristics associated with foliation. Laboratory test data (5) show three mutually orthogonal material directions that are perpendicular to foliation, parallel to foliation down dip, and parallel to foliation along strike.

The rock is orthogonally anisotropic; nine independent moduli characterize the elasticity of each formation. The principal values of Young's modulus in the Poorman Formation range from 7.2×10^6 psi perpendicular to the foliation to 13.7×10^6 psi parallel to foliation. Young's modulus at an angle to the foliation may be greater or less than the principal values. The same is true of the shear modulus. Poisson's ratios range from 0.15 to 0.23.

Foliation is least pronounced in the Homestake Formation; principal values of Young's modulus range between 9.0×10^6 and 12.8×10^6 psi, and Poisson's ratios range between 0.14 and 0.19.

If the rock were isotropic, then a higher Young's modulus (greater than 6.5×10^6 psi) would be justified in the data reduction computations. However, it is possible that there is a relative maximum or minimum modulus at angles to the foliation and that some values fall outside the range given here. The assumption of isotropy and its effect on the in situ stress state must therefore await a more detailed analysis and a data reduction scheme that accounts for anisotropy. Amadei (6) has proposed such a scheme, but a field measurement procedure has not been established as a standard practice.

DATA REDUCTION USING LEAST SQUARES APPROACH

The least squares, best fit approach to calculating in situ stresses from the measured HICell strains is not necessarily the best one. Substantial differences in stresses may occur between the first trial using data from all nine gauges in a HICell and the third, "best fit" trial using data from only six gauges. The best fit stress state is thus a result based on a purely statistical criterion.

An alternative view guided by rock mechanics principles (7) is to average the axial strain measurements before proceeding to an analytical estimate of the three normal stresses and the shear stress σ_{xx} , σ_{yy} , σ_{zz} , and σ_{xy} in a plane perpendicular to the borehole axis (the z-axis). The z-direction shear stresses σ_{yz} and σ_{zx} can then be estimated from the three shear strains calculated from the three three-gauge rosettes in a HICell. The latter calculation may be expressed analytically as a least squares fit of the two shear stresses to the three measurements.

The alternative approach is based on average axial strains and may lead to significant differences in results when the axial strains are substantially different from one another. A theoretical analysis of strain relief using over-coring shows that the axial strains are independent of position about the circumference of the HICell. Ideally, the axial strain measurements should be equal in isotropic rock. Indeed, a criterion for measurement validity could be based on equality of the axial strains. In actual practice, it would be quite unusual if the axial strains were equal; averaging the axial strains seems reasonable. An

unanswered question is how different the axial strains can be before the data are deemed invalid.

The data presented in table 5 illustrate the effects of different treatments of axial strain in the reduction of the HICell data from site 2. The four K-factors⁹ used in the data reduction were set to 1 for the comparisons. Inspection of the results given in table 5 show that reversal of normal stress ordering relative to data from site 1 was present in the original least squares, best fit approach. The results using the high values of axial strain are quite close to results from the original analysis. The reason is that the low value is eliminated during the process of obtaining a best fit. However, the reversal does not occur when the axial strains are averaged before the least squares approach is applied. Averaging not only removes the reversal, but substantially reduces the north-south stress as well. The same results occur when the low value of axial strain in the site 2 data are used. The results from axial strain averaging from site 2 are much closer to those from site 1 (table 3).

Table 5.—Different axial strain treatments and results from site 2, pounds per square inch
(Compressive stress is positive)

Treatment	Normal			Shear		
	North-south	East-west	Vertical	North-south and east-west	East-west and vertical	North-south and vertical
Original	4,442	2,658	5,789	-105	787	-735
Low	2,862	2,978	5,684	-199	710	-534
Average	2,649	2,964	5,639	417	698	-878
High	4,273	2,536	5,706	-221	853	-567

SUMMARY AND CONCLUSIONS

The measured and calculated shaft pillar stresses at site 1 and measured stresses at site 2 are summarized in table 6. Although the data are sparse, several conclusions seem justified.

1. The measured normal stresses at site 1 are less than those estimated from finite-element simulations of actual mining. The finite-element results are therefore pessimistic and somewhat conservative.

2. Differences in normal stresses between sites 1 and 2 are the same magnitude as differences within site 1, so that horizontal gradients of normal stress between sites 1 and 2 cannot be determined reliably. The shear stresses

are an order of magnitude smaller than the normal stresses and show a considerable percentage variation that masks the smaller absolute differences.

A more detailed investigation of the physical appropriateness of the least squares, best fit approach seems warranted. Also needed is a more elaborate analysis of axial strain effects on the data reduction procedure for anisotropic rock.

⁹K-factors are defined as correction factors that compensate for the gap between the rock and the strain gauges (4).

Table 6.—Stresses near Ross shaft pillar at sites 1 and 2, pounds per square inch

(Compressive stress is positive)

Site and calculation	Normal			Shear		
	North-south	East-west	Vertical	North-south and east-west	East-west and vertical	North-south and vertical
SITE 1						
Arithmetic average	2,357	3,735	4,167	189	-597	-453
Finite-element model	2,577	4,882	6,135	-258	76	256
SITE 2						
Axial strain average	2,649	2,964	5,639	417	698	-878

REFERENCES

1. Pariseau, W. G. Research Study on Pillar Design for Vertical Crater Retreat (VCR) Mining (contract JO215043, Univ. UT). BuMines OFR 44-86, Oct. 1985, 233 pp.; NTIS PB 86-210960.
2. Jenkins, F. M., and R. W. McKibbin. Practical Considerations of In Situ Stress Determination. Paper in Application of Rock Characterization Techniques in Mine Design (ed. by M. Karmis). Soc. Min. Eng. AIME, Littleton, CO, 1986, pp. 33-39.
3. Commonwealth Scientific and Industrial Research Organization (Warwick, Queensland, Aust.). Field Manual C.S.I.R.O. HI Stress Gage. 1983, 98 pp.; distributed by Geokon, W. Lebanon, NH.
4. Larson, M. K. STRESsOUT—A Data Reduction Program for Inferring Stress State of Rock Having Isotropic Material Properties: A User's Manual. BuMines IC 9302, 1992, 163 pp.
5. Duan, F. Numerical Assessment of the Importance of Anisotropy to Steeply Dipping Vertical Crater Retreat Stopes. M.S. Thesis, Univ. UT, 1986, 178 pp.
6. Amadei, B. Rock Anisotropy and the Theory of Stress Measurements. Springer-Verlag, New York, NY, 1983, 478 pp.
7. Duncan Fama, M. E., and M. J. Pender. Analysis of the Hollow Inclusion Technique for Measuring In Situ Rock Stress. Int. J. Rock Mech. Min. Sci. & Geomech. Abstr., v. 17, 1980, pp. 137-146.

APPENDIX A.—OVERCORE STRAIN DATA FROM HOLLOW INCLUSION CELLS

Figure A-1 shows the overcore strain data collected for each HICell measurement. The abscissa (horizontal axis) is the distance between the drill bit and the centerline of the rosettes measured in inches. Negative values indicate the bit was approaching the gauges, while positive values

mean the bit had passed the gauges. The ordinate (vertical axis) is the measured value of strain in units of microstrain. Oscillations of measured strain from gauge 9 in these plots is probably a fault in the recording channel.

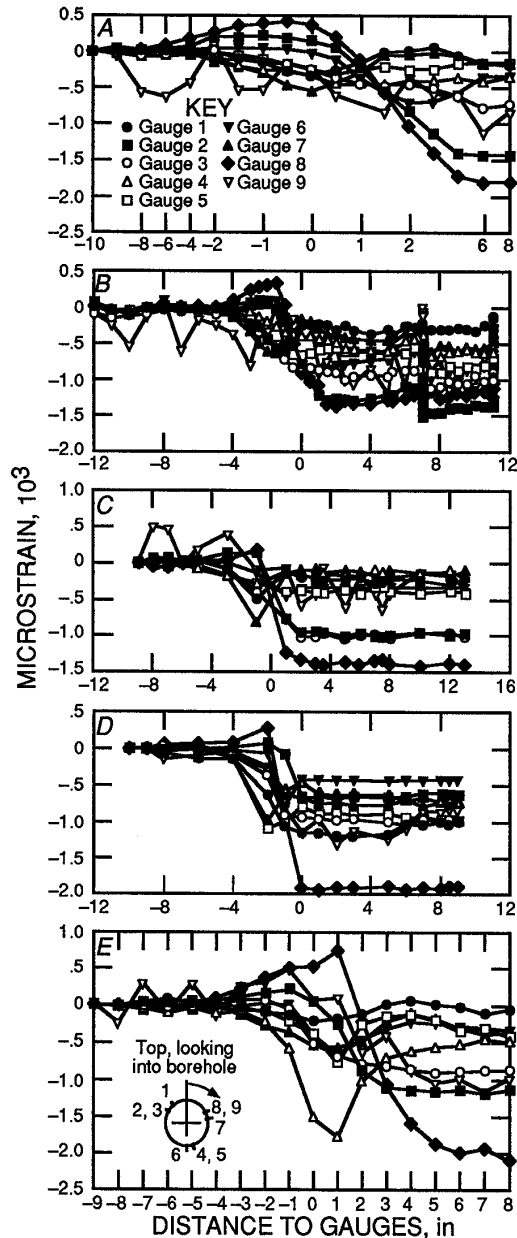


Figure A-1.—Overcore readings from HICells. A, S1H1C1; B, S1H2C1; C, SH3C1; D, S1H3C2; E, S2H1C1.

APPENDIX B.—OVERCORE PLOTS FROM BOREHOLE DEFORMATION GAUGES

Figure B-1 shows the overcoring response of BDG at site 1 for boreholes 1, 2, and 3. Again, the abscissa is the distance between the drill bit and the centerline of the

gauge; however, the ordinate represents the change in the diameter of the borehole as measured in inches.

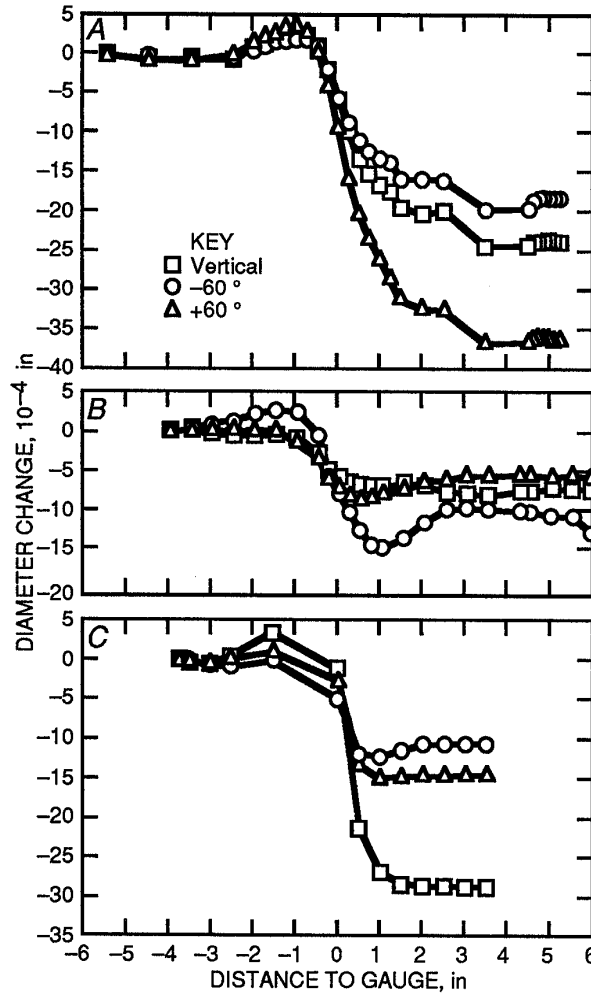


Figure B-1.—Response of BDG to mining, site 1. A, Hole 1; B, hole 2; C, hole 3.